X-dependent electronic structure of $YbXCu_4$ (X = In, Cd, Mg) investigated by high-resolution photoemission spectroscopy

2002 J. Phys.: Condens. Matter 14 4445

(http://iopscience.iop.org/0953-8984/14/17/316)

INSTITUTE OF PHYSICS PUBLISHING JOURNAL OF PHYSICS: CONDENSED MATTER

J. Phys.: Condens. Matter **14** (2002) 4445–4459 PII: S0953-8984(02)33122-9

X-dependent electronic structure of $YbXCu_4$ (X = In, Cd, Mg) investigated by high-resolution photoemission spectroscopy

H Sato[1,5], K Hiraoka[2], M Taniguchi[1,3], Y Nishikawa[1], F Nagasaki[1], H Fujino[1], Y Takeda[1,6], M Arita[3], K Shimada[3], H Namatame[3], A Kimura[1] and K Kojima[4]

[1] Graduate School of Science, Hiroshima University, Kagamiyama 1-3-1, Higashi-Hiroshima 739-8526, Japan
[2] Faculty of Engineering, Ehime University, Bunkyo-cho 3, Matsuyama 790-8577, Japan
[3] Hiroshima Synchrotron Radiation Centre, Hiroshima University, Kagamiyama 2-313, Higashi-Hiroshima 739-8526, Japan
[4] Faculty of Integrated Arts and Sciences, Hiroshima University, Kagamiyama 1-7-1, Higashi-Hiroshima 739-8521, Japan

E-mail: jinjin@hiroshima-u.ac.jp

Received 28 January 2002
Published 18 April 2002
Online at stacks.iop.org/JPhysCM/14/4445

Abstract

Valence-band electronic structure of $YbXCu_4$ (X = In, Cd, Mg) has been investigated by means of high-energy-resolution photoemission spectroscopy with an He I resonance line ($h\nu = 21.22$ eV) from 10 to 300 K. In the photoemission spectra of $YbInCu_4$ and $YbCdCu_4$ near the Fermi level (E_F) measured at 10 K, the prominent peak structures due to the Yb^{2+} $4f_{7/2}$ states are clearly observed at 46 and 31 meV, respectively. The difference of the peak energies qualitatively reflects that of the Kondo temperatures between $YbInCu_4$ and $YbCdCu_4$. The peak intensities increase gradually with decreasing temperature for both compounds. The amount of enhancement of the Yb^{2+} $4f_{7/2}$ peak from 50 to 10 K is, however, much stronger for $YbInCu_4$ than for $YbCdCu_4$, due to an increase of the Yb^{2+} component followed by the valence transition at $T_v = 42$ K in $YbInCu_4$. On the other hand, the Yb^{2+} $4f_{7/2}$ states of $YbMgCu_4$ is observed as a broad structure near E_F in the photoemission spectrum at 10 K. We have also measured the x-ray photoemission spectra in the Yb 4d core state region of $YbXCu_4$ from 10 to 300 K. For $YbInCu_4$ and $YbCdCu_4$, the structures due to the Yb^{2+} and Yb^{3+} components are recognized for all temperatures. In particular, the Yb^{2+} structure is still observed at 300 K for $YbInCu_4$. The intensity ratio of Yb^{2+}/Yb^{3+} increases gradually with decreasing temperature for both compounds. For $YbMgCu_4$, on the other hand, almost only Yb^{2+} structures are observed and little temperature dependence is detected.

[5] Author to whom any correspondence should be addressed.
[6] Present address: Hiroshima Synchrotron Radiation Centre, Hiroshima University, Kagamiyama 2-313, Higashi-Hiroshima 739-8526, Japan.

1. Introduction

The ternary compounds $YbXCu_4$ (X = In, Ag, Au, Pd, Cd, Mg, Tl, Zn) with a cubic $C15b$-type structure exhibit a wide variety of physical properties [1, 2]. $YbAgCu_4$ is a prototype heavy-fermion compound with γ above 200 mJ mol^{-1} K^{-2} with no magnetic ordering, where γ is a linear specific coefficient. $YbCdCu_4$ and $YbZnCu_4$ also exhibit heavy-fermion behaviour with γ of 175 and 230 mJ mol^{-1} K^{-2}, respectively. On the other hand, $YbAuCu_4$ orders magnetically below 1 K, and the low-temperature properties are dominated by Ruderman–Kittel–Kasuya–Yoshida interactions and crystal field effects. $YbPdCu_4$ also orders magnetically below 1 K.

Among these ternary compounds, $YbInCu_4$ has, in particular, attracted the greatest interest and been most extensively studied so far. This compound exhibits a first-order isostructural valence transition at $T_v = 42$ K [3–5]. At high temperature, Yb is nearly trivalent, displaying Curie–Weiss susceptibility with paramagnetic moment near the free-ion value of 4.5 μ_B. At T_v, the Yb valence is reduced to 2.8 and the magnetic susceptibility shows a temperature-independent Pauli paramagnetism. The lattice volume changes by 0.5% at the transition, but there is no change in the cubic $C15b$ crystal symmetry. Such an 'isomorphic' valence transition is fundamentally similar to the α–γ transition in Ce [6,7]. Furthermore, the Kondo temperature changes from $T_{K+} \sim 25$ K at high temperature to $T_{K-} \sim 400$ K at low temperature [8]. The mechanism of the valence transition has not been clearly revealed yet and is still under investigation [9].

The direct investigation of the electronic structure, in particular the Yb 4f states of $YbInCu_4$, has been carried out extensively by means of temperature-dependent photoemission spectroscopy using synchrotron radiation [10–14]. Reinert *et al* [12] reported a detailed temperature dependence of a peak intensity of the Yb^{2+} $4f_{7/2}$ states near the Fermi level (E_F). The peak intensity does not show a critical change at the valence transition and increases continuously with decreasing temperature even through T_v. The authors proposed that the subsurface zone is important for $YbInCu_4$. On the other hand, Moore *et al* [14] reported that the peak intensities of the Yb^{2+} $4f_{7/2}$ and $4f_{5/2}$ states show a critical change just corresponding to the valence transition. However, there are still some controversies on the analyses and explanations of the photoemission results for $YbInCu_4$ [15, 16]. As concerns $YbAgCu_4$, $YbAuCu_4$ and $YbPdCu_4$, their photoemission spectra using an Al Kα line have been compared at 110 K with the experimental energy resolution of $\sim$1.2 eV [17]. Weibel *et al* [18] have also measured the photoemission spectra of $YbAgCu_4$ using the He resonance lines from 20 to 260 K with the resolution below 25 meV. For $YbCdCu_4$, $YbMgCu_4$, $YbZnCu_4$ and $YbTlCu_4$, added as new members of this family recently [1, 2, 19], the photoemission experiments have not been carried out so far.

The purpose of the present study is to investigate the X dependence of electronic structure of $YbXCu_4$. We report the valence-band electronic structure near E_F as well as in the wide binding-energy region of $YbInCu_4$, $YbCdCu_4$ and $YbMgCu_4$ by means of the high-energy-resolution ultraviolet photoemission spectroscopy in the temperature region from 10 to 300 K. We have also measured the x-ray photoemission spectra in the Yb 4d core state region. A comparison of experimental results of $YbInCu_4$ with those of $YbCdCu_4$ and $YbMgCu_4$ is fruitful to reveal the electronic structure peculiar to $YbInCu_4$, and furthermore is expected to provide a clue to understand the mechanism of the valence transition of $YbInCu_4$.

Valence electrons of X elements contribute to E_F of $YbXCu_4$ compounds and are expected to play an important role in determining a wide variety of their physical properties since their crystal structures are of the same $C15b$ type. Here, nominal electron configurations of the In and Cd elements in solids are $(4d)^{10}(5sp)^3$ and $(4d)^{10}(5sp)^2$, respectively. On the other

hand, the Mg element has the $(3sp)^2$ configuration. Comparisons of electronic structure of $YbInCu_4$ with that of $YbCdCu_4$ and $YbMgCu_4$ would provide information on how the number of electrons of the (5sp) orbitals and the principal quantum number n of the ($n$sp) orbitals of the X elements affect their physical properties[7].

$YbCdCu_4$ and $YbMgCu_4$ have been studied less so far. Hiraoka *et al* [19, 20] performed the ^{113}Cd NMR and ^{63}Cu NQR experiments on $YbCdCu_4$ and concluded that the Yb 4f states changes gradually from the Fermi liquid to localized states from low to high temperature. The magnetic field rather sensitively influences the Fermi liquid state in $YbCdCu_4$. The Kondo temperatures T_K of $YbCdCu_4$ and $YbMgCu_4$ are estimated to be ∼220 and ∼850 K, respectively, from the magnetic susceptibility experiments [1].

2. Experimental details

Angle-integrated high-resolution photoemission experiments for $YbXCu_4$ (X = In, Cd, Mg) were carried out using a hemispherical analyser (Gammadata-Scienta ESCA-200) with an energy resolution below 5 meV. As excitation photon sources, we used an He I resonance line ($h\nu = 21.22$ eV) from an intense He discharge lamp (Gammadata-Scienta VUV-5010) for valence-band photoemission experiments and a monochromatized Al Kα line ($h\nu = 1486.6$ eV) from an x-ray tube for the Yb 4d photoemission spectra. The temperature of the sample was controlled between 10 and 300 K using a flow-through cryostat with liquid helium and a heater attached to the sample holder. The clean surfaces of samples were obtained *in situ* by scraping with a diamond file every ∼30 min in the analysis chamber with a base pressure of $\sim 3 \times 10^{-10}$ Torr. Within 30 min no change of the spectra was observed. As for $YbInCu_4$, the photoemission spectra for the sample surfaces prepared by scraping and cleavage are compared in [12]. The temperature dependence of the spectra is the same for cleaved and scraped sample surfaces, though the Yb $4f_{7/2}$ peak intensity is slightly weaker for the scraped surface. In this paper, we limit the discussion to the temperature dependence and X dependence of the photoemission spectra[8,9]. Binding energy of the photoemission spectra is defined with respect to E_F of respective samples, which was determined from the Fermi edge of Au films evaporated directly onto the sample surfaces just after the measurements.

$YbInCu_4$ and $YbCdCu_4$ samples used for the present experiments were single crystals prepared by the flux growth method similar to that described by Sarrao *et al* [5]. The constituent elements with stoichiometric ratios in InCu or CdCu fluxes were put in an alumina crucible and sealed in an evacuated quartz ampoule. The sample was then heated to 1100 °C and cooled slowly to 800 °C. After keeping at 800 °C for 20 h, the flux was removed. $YbMgCu_4$ samples were polycrystals. An appropriate amount of the elements was melted in the arc-furnace. After the reaction, the product in the quartz ampoule was annealed at 600 °C for two weeks. The crystal structures of all samples were confirmed to be the $C15b$ type by x-ray powder diffraction. As for $YbInCu_4$, the temperature width of the valence transition at $T_v = 42$ K was below 2 K from the measurements of the magnetic susceptibility.

[7] $YbAlCu_4$ and $YbGaCu_4$, where the Al and Ga elements in solids have the $(3sp)^3$ and $(4sp)^3$ configurations, respectively, have a hexagonal structure.

[8] Photoemission experiments for the cleaved surfaces and bulk-sensitive photoemission experiments using excitation photon energy below 10 eV are in progress.

[9] Also for $YbCdCu_4$, we assume no difference in temperature dependence between the surface preparations by scraping and cleaving.

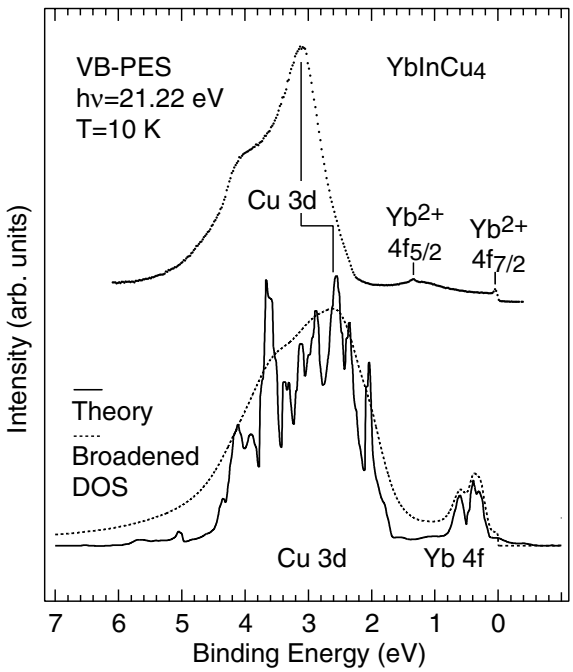

Figure 1. Valence-band photoemission spectrum of $YbInCu_4$ measured at 10 K (dots). The theoretical DOS derived from the band-structure calculation [21] and a broadened curve taking into account the experimental resolution and lifetime broadening are also shown as solid and dashed curves, respectively.

3. Results and discussion

The valence-band photoemission spectrum of $YbInCu_4$ measured with the He I resonance line at 10 K is shown by the dotted curve in figure 1. The density of states (DOS) derived from a band-structure calculation based on the self-consistent augmented plane wave method with the local density approximation is also shown by a solid curve [21]. A dashed curve represents a broadened DOS convoluted with the Gaussian and Lorentzian functions taking into account the experimental resolution and lifetime broadening, respectively[10], for a comparison between the experiment and theory. On the basis of the band-structure calculation, the Cu 3d states contribute to the valence bands from 2 to 5 eV with the most prominent doublet structure: a main peak around 3 eV and a shoulder around 4 eV. The theoretical DOS feature reproduces well the experimental spectrum. The energy position of the Cu 3d structure in the experimental spectrum is, however, deeper than the theory by 0.6 eV. The feature of the Yb^{2+} 4f states near E_F is completely different between the experiment and theory, because the spin–orbit splitting of the Yb 4f states is eliminated in the theory. In the experimental spectrum, the Yb^{2+} $4f_{7/2}$ states are recognized just below E_F and the Yb^{2+} $4f_{5/2}$ states around 1.35 eV.

In figure 2, we compare the valence-band photoemission spectra of $YbXCu_4$ (X = In, Cd, Mg) measured at 10 K. The binding energy of the main peak due to the Cu 3d states of $YbInCu_4$ is 3.1 eV, while those of $YbCdCu_4$ and $YbMgCu_4$ are 3.0 eV. The energy difference of the Cu 3d structure is qualitatively understood by taking into account the number of valence

[10] The full width at half maximum (FWHM) of the Gaussian function is assumed to be 10 meV and the binding-energy-(E_B-)dependent FWHM of the Lorentzian function to be $2\Gamma = 0.15\ E_B + 0.01$ eV.

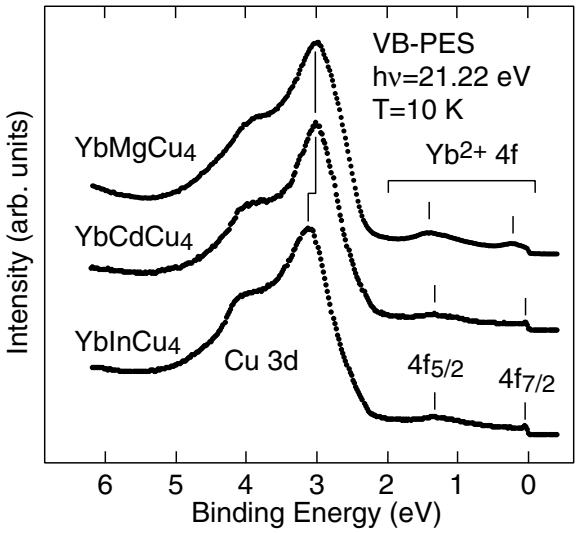

Figure 2. Valence-band photoemission spectra of $YbXCu_4$ (X = In, Cd, Mg) measured at 10 K. The energy position of the main peak due to the Cu 3d states shifts according to the X-element positions in the periodic table. The structure due to the Yb^{2+} 4f states is different only for $YbMgCu_4$.

electrons of the In, Cd and Mg elements. The Cd atom is located just on the left of the In atom in the periodic table and the Mg atom may be placed above Zn and Cd atoms. The number of valence electrons of the Cd and Mg atoms, which form the conduction bands (CBs) around E_F in the compound, is smaller than that of the In atom nominally by one per atom. On the assumption of the almost constant DOS around E_F among the three compounds, the difference of the number of valence electrons would change the E_F position within the CBs. Thus, the energies of the Cu 3d states of $YbCdCu_4$ and $YbMgCu_4$ are not so different with respect to E_F, and would be shallower in comparison with that of $YbInCu_4$. In fact, the Cu 3d structure in the photoemission spectra of $YbAgCu_4$, where the number of valence electrons of the Ag atom is again smaller than those of the Cd and Mg atoms nominally by one per atom, is located around 2.9 eV [18].

Here, we present the temperature dependence of the photoemission spectra near E_F with the peak due to the Yb^{2+} $4f_{7/2}$ states of $YbInCu_4$ and $YbCdCu_4$ measured from 10 to 300 K in figure 3. The spectra are normalized using intensities in the binding-energy region of 150–300 meV. Roughly speaking, the temperature dependence of the Yb^{2+} $4f_{7/2}$ peak of both compounds is similar. The peak intensity becomes strong and the peak energy shifts gradually toward the E_F side with decreasing temperature. The peak is hardly observed at 300 K. Similar temperature dependence has also been observed for $YbAgCu_4$ [18] and $YbAl_3$ [22]. One notices, however, some differences between the temperature dependences of the Yb^{2+} $4f_{7/2}$ peak of the two compounds. The Yb^{2+} $4f_{7/2}$ peak energies of $YbInCu_4$ and $YbCdCu_4$ at 10 K are around 50 and 30 meV, respectively. For $YbCdCu_4$, the peak energy shifts gradually toward the E_F side with decreasing temperature. For $YbInCu_4$, on the other hand, the peak energy first shifts gradually toward the E_F side from 300 to 50 K and then shifts slightly to the deeper-binding-energy side from 50 to 10 K in contrast to the results of $YbCdCu_4$. Furthermore, the enhancement of the peak intensity from 50 to 10 K for $YbInCu_4$ is much remarkable than that for $YbCdCu_4$.

The curve fittings of the photoemission spectra near E_F in figure 3 were carried out. A representative result is shown in figure 4 for the spectrum of $YbInCu_4$ at 10 K. We assume that

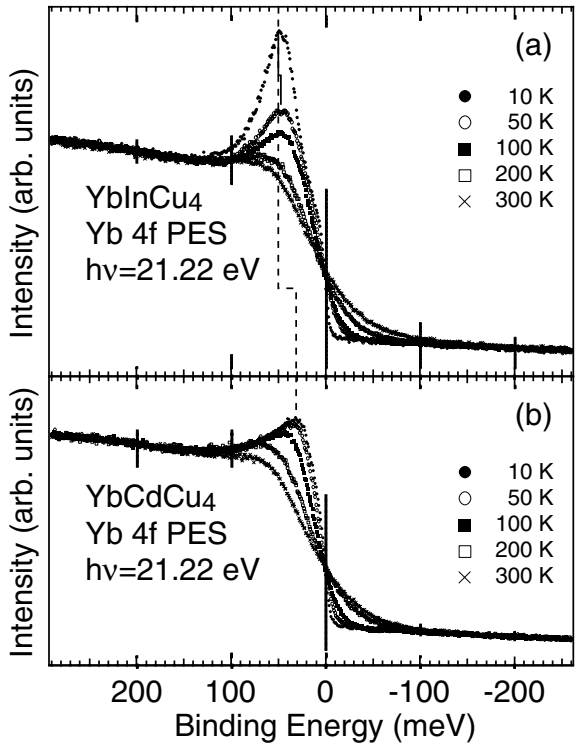

Figure 3. Photoemission spectra near E_F of (*a*) $YbInCu_4$ and (*b*) $YbCdCu_4$ measured at 10, 50, 100, 200 and 300 K. For both compounds, the Yb^{2+} $4f_{7/2}$ peak is clearly observed at 10 K. With decreasing temperature, the peak intensity increases and the peak energy shifts towards the E_F side. The amount of enhancement of the peak intensity from 50 to 10 K is far greater for $YbInCu_4$ than for $YbCdCu_4$.

the experimental spectra consist of the structures due to the Yb^{2+} $4f_{7/2}$ states, the CBs and the background contributions caused by secondary electrons. The asymmetric Doniach–Sunjic line shape [23] is used to represent the Yb^{2+} $4f_{7/2}$ feature [11, 24]. The CBs are assumed to be structureless with constant DOS for all temperatures, and the Shirley method [25] is adopted to evaluate the background contribution due to secondary electrons. Finally, we convolute the summed curve with the Gaussian function to represent the experimental resolution, after taking into account the thermal broadening using the Fermi–Dirac function. The derived curves reproduce well the experimental results. For the other spectra of $YbInCu_4$ and also $YbCdCu_4$, the fitting procedure works successfully. For both compounds, values of a singularity index α decrease with decreasing temperature: $\alpha = 0.37$ (300 K) to 0.15 (10 K) for $YbInCu_4$ and $\alpha = 0.43$ (300 K) to 0.29 (10 K) for $YbCdCu_4$. Here α is proportional to the square of the phase shift for scattering of conduction electrons from the hole potential and reflects the asymmetry index of the line shape.

From the fitting procedure, we have estimated the intensity and energy position of the Yb^{2+} $4f_{7/2}$ peak in the temperature-dependent photoemission spectra near E_F. Figure 5 shows the Yb^{2+} $4f_{7/2}$ peak intensities of $YbInCu_4$ and $YbCdCu_4$ as a function of temperature, which are normalized to that at 300 K for respective samples. One notices that the peak intensity of $YbCdCu_4$ increases continuously with decreasing temperature down to 10 K. For $YbInCu_4$ from 300 to 50 K, on the other hand, the intensity also increases continuously, similar to the

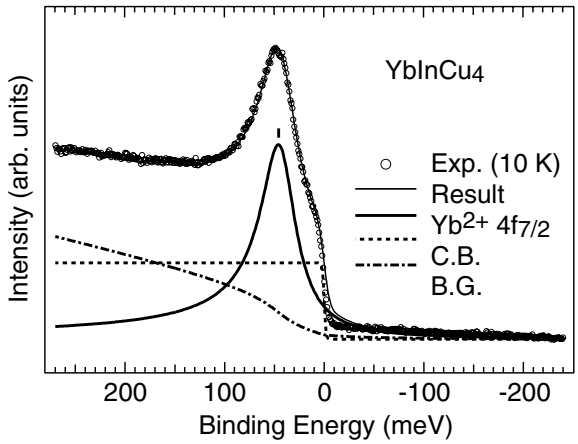

Figure 4. Fitting results of the photoemission spectrum of $YbInCu_4$ measured at 10 K with the Yb^{2+} $4f_{7/2}$ states, structureless CBs and background (BG) due to the secondary electrons taking into account the thermal broadening. For the other spectra of $YbInCu_4$ and also $YbCdCu_4$, the fitting procedure works well successfully. (See the text.)

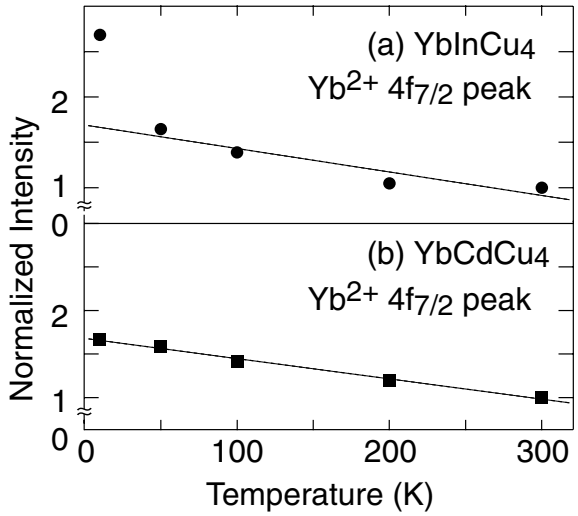

Figure 5. The Yb^{2+} $4f_{7/2}$ peak intensities in the photoemission spectra of (*a*) $YbInCu_4$ and (*b*) $YbCdCu_4$ as a function of temperature. The peak intensities increase with decreasing temperature. The amount of enhancement from 50 to 10 K is greater for $YbInCu_4$ than for $YbCdCu_4$.

results of $YbCdCu_4$, while from 50 to 10 K the intensity is significantly enhanced compared with $YbCdCu_4$.

Figure 6 shows the temperature dependence of the Yb^{2+} $4f_{7/2}$ peak energies of $YbInCu_4$ and $YbCdCu_4$ as a function of temperature. One notices again that the peak energy shifts gradually toward the E_F side from 300 to 50 K for both compounds. The temperature dependence from 50 to 10 K is, however, different between the two compounds. In the case of $YbCdCu_4$ the peak energy shifts monotonically toward the E_F side also down to 10 K, while in the case of $YbInCu_4$ the peak energy shifts to the deeper-binding-energy side, in contrast to the trend from 300 to 50 K.

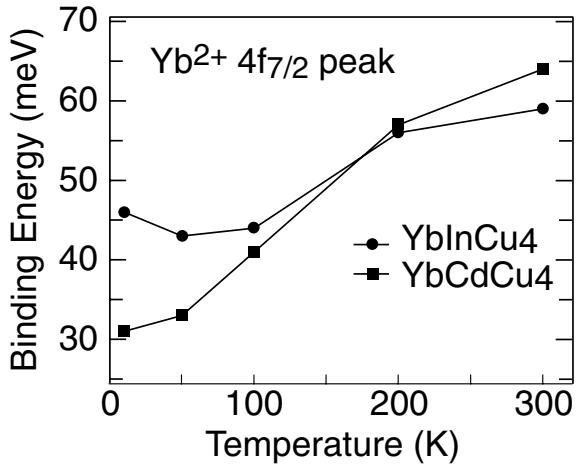

Figure 6. The Yb^{2+} $4f_{7/2}$ peak energies in the photoemission spectra of $YbInCu_4$ and $YbCdCu_4$ as a function of temperature. The energies shift gradually toward the E_F side down to 50 K for both compounds. The temperature dependence from 50 to 10 K is different between two compounds. The peak energy at 10 K reflects T_K qualitatively.

According to the single-impurity Anderson (SIA) model, the Yb^{2+} $4f_{7/2}$ peak, commonly called the Kondo resonance, is placed at the binding energy of $k_B T_K$ in the photoemission spectra at $T = 0$ K [18, 26]. The peak energies of $YbInCu_4$ and $YbCdCu_4$ at 10 K are 46 and 31 meV, respectively, corresponding to 534 and 360 K. The deeper peak energy for $YbInCu_4$ is, thus, qualitatively consistent with the higher T_K-value: ∼430 K for $YbInCu_4$ [5] and ∼220 K for $YbCdCu_4$ [1] from the magnetic susceptibility experiments.

The remarkable enhancement of the peak intensity and the energy shift to the deeper-binding-energy side observed for $YbInCu_4$ from 50 to 10 K is assumed to be peculiar to this compound. These experimental results have not been observed for $YbAgCu_4$ [18] or $YbAl_3$ [22]. The remarkable enhancement of the Yb^{2+} $4f_{7/2}$ peak intensity indicates that the Yb^{2+} component increases due to the valence transition. The energy shift is also qualitatively understood from the change of T_K: $T_{K+} \sim 25$ K in the high-temperature region to $T_{K-} \sim 400$ K in the low-temperature region [8]. Thus the different temperature dependences for the Yb^{2+} $4f_{7/2}$ peak of $YbInCu_4$ between 50 and 10 K from those for $YbCdCu_4$ and $YbAgCu_4$ [18] would be attributed to the change of the electronic structure through the valence transition at $T_v = 42$ K.

From the change of T_K (ΔT_K) at the valence transition of $YbInCu_4$, one would expect an energy shift of the Yb^{2+} $4f_{7/2}$ peak to the deeper-binding-energy side in the low-temperature region of about $k_B \Delta T_K \sim 32$ meV with $\Delta T_K \sim 375$ K ($T_{K+} \sim 25$ K and $T_{K-} \sim 400$ K). The value of the energy shift between 10 and 50 K (figure 6) is, however, ∼3 meV and is far smaller, by an order of magnitude, than the expected value. Quantitative explanations based on the SIA model should be re-examined [18, 22].

In the high-temperature region of $YbInCu_4$, $T_{K+} \sim 25$ K provides $k_B T_{K+} \sim 2$ meV, which might be too shallow a binding energy to detect correctly from the Yb^{2+} $4f_{7/2}$ peak in the photoemission spectra due to the experimental resolution and thermal effects. Also for the Yb^{2+} $4f_{5/2}$ peak at 1.35 eV, the photoemission spectra of $YbInCu_4$ in the high- and low-temperature regions have been calculated from the Gunnarsson–Schönhammer method [13,14]. The calculated energy shift of the Yb^{2+} $4f_{5/2}$ peak is also ∼32 meV. Figure 7 shows the

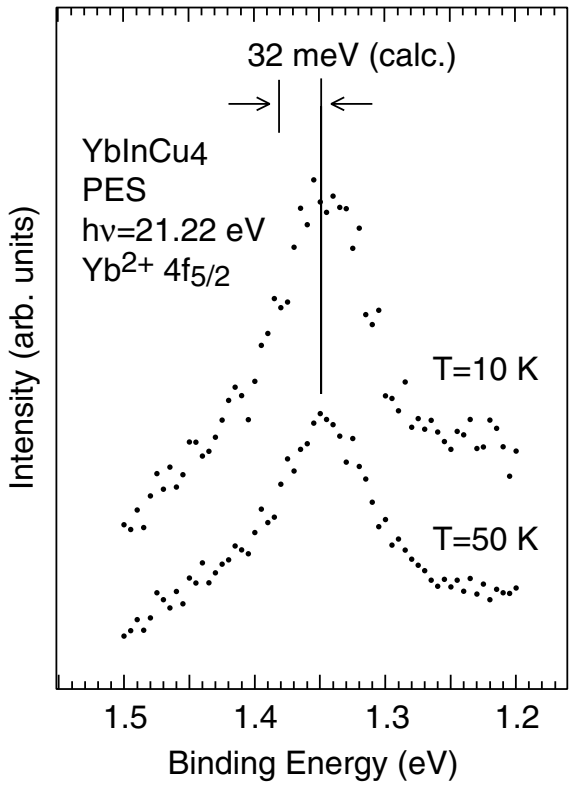

Figure 7. Photoemission spectra in the Yb^{2+} $4f_{5/2}$ peak region of $YbInCu_4$ measured at 10 and 50 K. The energy shift with a value of about 32 meV, derived from the calculated photoemission spectra using the Gunnarsson–Schönhammer method, has not been observed.

photoemission spectra in the Yb^{2+} $4f_{5/2}$ peak region of $YbInCu_4$ measured at 10 and 50 K. Although the value of the energy shift of ∼32 meV is sufficiently detectable within the experimental resolution, almost no energy shift for the Yb^{2+} $4f_{5/2}$ peaks is observed, in agreement with the photoemission results by Joyce *et al* [13] and Moore *et al* [14].

Figure 8 shows the photoemission spectra of $YbXCu_4$ (X = In, Cd, Mg) near E_F measured at 10 K. The spectra are normalized using intensities in the binding-energy region of 300–700 meV, where we assume a dashed line between 350 and 550 meV for the spectra of $YbInCu_4$ and $YbCdCu_4$. The peak intensity of $YbInCu_4$ is stronger compared with that of $YbCdCu_4$, suggesting that the Yb atom in $YbInCu_4$ is more trivalent than that in $YbCdCu_4$ at 10 K. The Yb^{2+} $4f_{7/2}$ structure of $YbMgCu_4$ is, on the other hand, extremely broad over the top ∼500 meV region compared with those of $YbInCu_4$ and $YbCdCu_4$. This indicates that the electronic structure near E_F of $YbMgCu_4$ is substantially different and the Yb^{2+} $4f_{7/2}$ states have a large dispersion due to the hybridization between the Yb^{2+} 4f and CB states.

Figure 9 shows the photoemission spectra near E_F of $YbMgCu_4$ measured from 10 to 300 K. Although the spectra are almost independent of temperature with respect to the broad feature of the Yb^{2+} $4f_{7/2}$ structure, the integrated peak intensity increases with decreasing temperature, similar to results for $YbInCu_4$ and $YbCdCu_4$. As concerns the centre of gravity of the peak, it rather shifts to the deeper-binding-energy side with decreasing temperature. The broad structure might be related to the high T_K of ∼850 K [1].

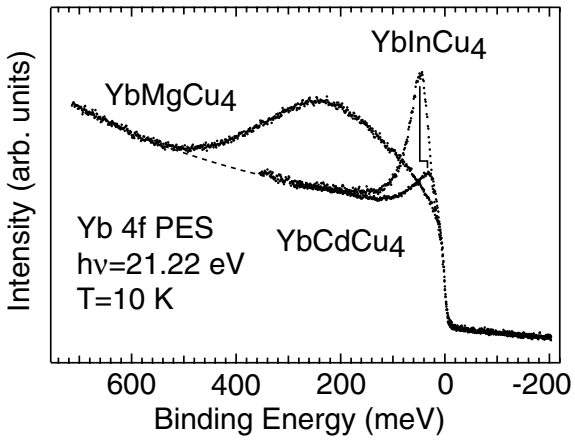

Figure 8. Photoemission spectra near E_F of $YbXCu_4$ (X = In, Cd, Mg) measured at 10 K. Only the Yb^{2+} $4f_{7/2}$ structure in the spectra of $YbMgCu_4$ is different from those of the other two compounds. Yb^{2+} $4f_{7/2}$ states in $YbMgCu_4$ have a large dispersion.

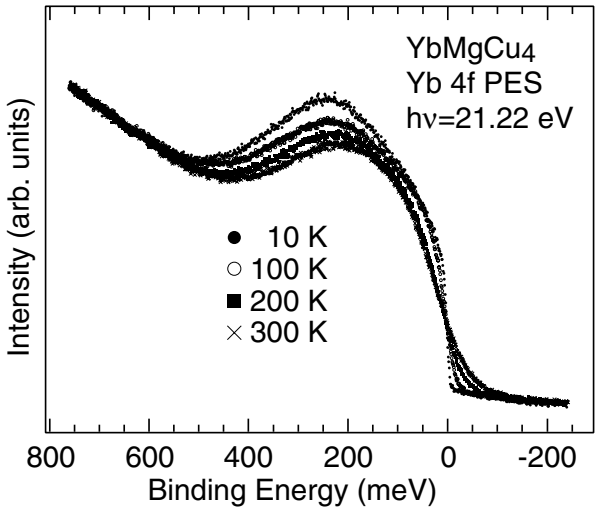

Figure 9. Photoemission spectra near E_F of $YbMgCu_4$ measured from 10 to 300 K. The integrated Yb^{2+} $4f_{7/2}$ peak intensity increases with decreasing temperature.

Here we comment on the photo-ionization cross section of the Yb 4f states. At $h\nu = 21.22$ eV, the Yb 4f cross section is extremely small compared with the other states forming the CBs such as the In 5p and Yb 5d states [27]. In fact, we have measured the photoemission spectra of $LuMgCu_4$ with the He I resonance line (not shown here) and the corelike Lu 4f states around 6 eV have hardly been observed. Therefore, to observe the Yb 4f components clearly, we have already measured the soft x-ray photoemission spectra at $h\nu = 800$ eV for the three compounds studied here and obtained results consistent with the present paper [28].

The valence-band photoemission spectra discussed above provide information only on the Yb^{2+} states. In order to investigate the temperature dependence of the Yb^{3+} states as well as

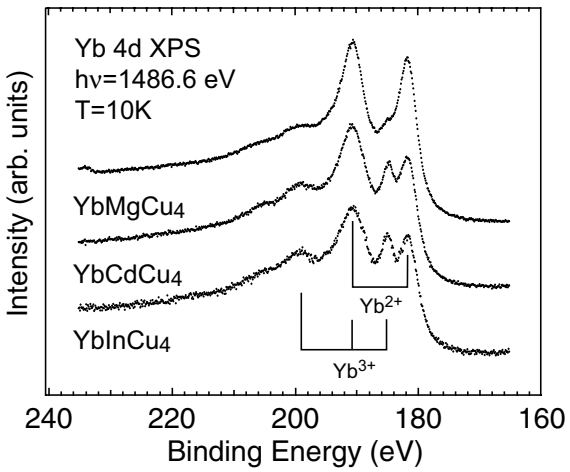

Figure 10. X-ray photoemission spectra in the Yb 4d core state region of $YbXCu_4$ (X = In, Cd, Mg) measured at 10 K. The spectra of $YbInCu_4$ and $YbCdCu_4$ show both Yb^{2+}- and Yb^{3+}-derived structures, while that of $YbMgCu_4$ almost only Yb^{2+}-derived structures.

the Yb^{2+} states, we have measured the x-ray photoemission spectra in the Yb 4d core state region using the Al Kα line. Figure 10 shows the Yb 4d spectra of $YbXCu_4$ (X = In, Cd, Mg) measured at $T = 10$ K. The multiplet structures around 181.5, 184.5, 190.5, 198.5 and 205 eV are observed for $YbInCu_4$ and $YbCdCu_4$. As for $YbMgCu_4$, the peak structures around 181.5 and 190.5 eV are remarkable.

A Yb 4d spectrum of compounds with the Yb^{2+} component is composed only of two peaks due to the spin–orbit splitting of the Yb 4d states. On the other hand, in the case of compounds with the Yb^{3+} component, the Yb 4d spectrum shows multiplet structures due to the Coulomb interaction between the 4d core hole and 4f electrons. In comparison with the Yb 4d spectra of YbAs (trivalent), $YbAl_3$ (mixed-valent) and $YbPd_3$ (divalent) [29], the peaks at 181.5 and 190.5 eV are attributed to the Yb^{2+} 4d states, while those at 184.5, 190.5 and 198.5 eV to the Yb^{3+} 4d states in figure 10. The Yb 4d spectra of $YbInCu_4$ and $YbCdCu_4$ exhibit both Yb^{2+} and Yb^{3+} components and almost only two peaks for $YbMgCu_4$. The Yb 4d spectrum indicates that the Yb atom in $YbMgCu_4$ is in a nearly divalent state, though the Yb^{3+}-derived structures are slightly observed. These experimental results for $YbXCu_4$ (X = In, Cd, Mg) with respect to the mixed divalent and trivalent states are in qualitative agreement with those of the Yb L_{III}-edge absorption experiments [1, 3], although the Yb^{3+} component in $YbMgCu_4$ is too small in the Yb 4d spectrum compared with the Yb L_{III}-absorption experiments, where the Yb valence at $\sim$10 K is estimated to be 2.37 [1].

Figure 11 shows a portion of the Yb^{2+}- and Yb^{3+}-derived peaks in the Yb 4d photoemission spectra of $YbInCu_4$ and $YbCdCu_4$ measured at 10, 50, 100, 200 and 300 K. The Yb^{2+} 4d peak intensities increase gradually, similar to the temperature dependence of the Yb^{2+} $4f_{7/2}$ peak intensity. On the other hand, the Yb^{3+} component decreases with decreasing temperature from 300 to 10 K in agreement with the increase of the Yb^{2+} component. It should be noticed that the Yb^{2+} component still exists at 300 K, which is also suggested from the Yb L_{III}-absorption experiments [3]. Although the relative component ratio of Yb^{2+}/Yb^{3+} in $YbInCu_4$ and $YbCdCu_4$ compounds increases gradually with decreasing temperature, the remarkable change caused by the valence transition of $YbInCu_4$ is not clearly observed.

Figure 12 shows the temperature dependence of the Yb 4d spectra of $YbMgCu_4$ between 10 and 300 K. In contrast to the results for $YbInCu_4$ and $YbCdCu_4$, the Yb 4d photoemission

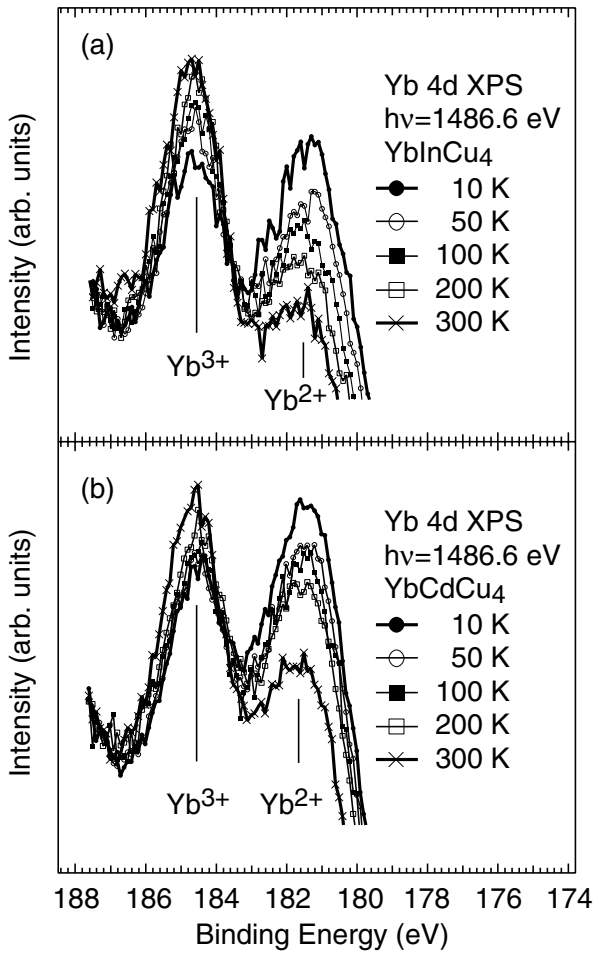

Figure 11. A portion of the Yb^{2+}- and Yb^{3+}-derived peaks in the Yb 4d photoemission spectra of $YbXCu_4$ (X = In, Cd, Mg) measured at 10, 50, 100, 200 and 300 K. With decreasing temperature, the intensity of the Yb^{2+} peaks increases gradually while that of the Yb^{3+} peaks decreases gradually.

spectra of $YbMgCu_4$ do not exhibit the noticeable temperature dependence. The Yb^{3+} 4d peak is, however, slightly observed at 190.5 eV in the Yb 4d spectrum at 300 K. Although the temperature dependence for $YbMgCu_4$ is much smaller than those for $YbInCu_4$ and $YbCdCu_4$, the gradual Yb valence change from the trivalent to divalent states with decreasing temperature is similar.

Finally, we discuss the X dependence of the electronic structure of $YbXCu_4$. The temperature dependence of the Yb^{2+} $4f_{7/2}$ and Yb 4d photoemission spectra of $YbInCu_4$ and $YbCdCu_4$ indicates that their electronic structure is similar. For both compounds, the amount of the Yb^{2+} component increases gradually with decreasing temperature. In addition, the valence-band photoemission spectra of $YbAgCu_4$ [18], where the Ag element in solids has nominally the $(5sp)^1$ electron configuration, exhibit the similar temperature dependence to those of $YbInCu_4$ and $YbCdCu_4$ with the $(5sp)^2$ In and $(5sp)^3$ Cd elements, respectively.

For three compounds, the Yb^{2+} $4f_{7/2}$ states are observed as the prominent peaks in the photoemission spectra near E_F. On the other hand, the energy positions of the Yb^{2+} $4f_{7/2}$

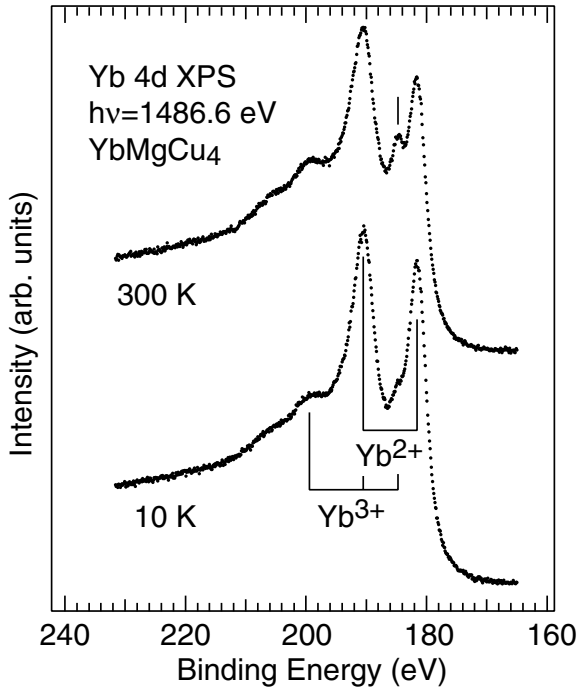

Figure 12. Yb 4d photoemission spectra of $YbMgCu_4$ measured at 10 and 300 K. The spectra do not show the noticeable temperature dependence so much. The Yb^{3+}-derived peak is slightly observed at 300 K.

peaks of $YbInCu_4$, $YbCdCu_4$ and $YbAgCu_4$ are 46 (at 10 K), 31 (at 10 K) and 22 meV (at 20 K, [18]), respectively. Although the Yb^{2+} $4f_{7/2}$ orbitals are corelike states, they hybridize slightly with the CB (c) states in $YbXCu_4$ compounds. Here we assume that the Yb^{2+} $4f_{7/2}$ states only in $YbInCu_4$ occupy a special energy position, leading a critical degree of c–f hybridization. With decreasing temperature, the degree of c–f hybridization increases due to the decrease of the lattice constant, which increases the Yb $4f^{14}$ (Yb^{2+}) from Yb $4f^{13}$ (Yb^{3+}) states. However, since the ionic radius of the Yb^{2+} ion is larger than that of the Yb^{3+} ion, the increase of the Yb^{2+} states competes with the decrease of the lattice constant. Therefore, at a critical temperature, the Yb^{2+} states increase suddenly with the lattice constant expansion, which would be more stable in total energy. In the case of $YbCdCu_4$ and $YbAgCu_4$, the situation of the competition between the Yb^{2+} ionic radius and the lattice constant is similar to that in the higher-temperature region of $YbInCu_4$ with $T_v = 42$ K still at 0 K, or the lower-temperature region still at high temperature just below the melting point. In order to confirm the above assumption, the experiments for $YbSnCu_4$ with the $(5sp)^4$ Sn elements, which is newly grown by Hiraoka, are in progress. The Yb^{2+} $4f_{7/2}$ states in $YbSnCu_4$ would be located at deeper energy than 46 meV and the situation of the competition is similar to the opposite temperature region of $YbInCu_4$ to those of $YbCdCu_4$ and $YbAgCu_4$.

In the case of $C15b$-type $YbMgCu_4$ with the $(3sp)^2$ Mg element, the Yb 4f states hybridize appreciably with CB states compared with $YbXCu_4$ with the $(5sp)^n$ X element, probably due to the different feature of the (3sp)- and (5sp)-derived CBs. The electronic structure shows little temperature dependence and the valence transition is no longer observed. We are also scheduled to carry out the experiments for $YbZnCu_4$ with the $(4sp)^2$ Zn element. We assume

that the (5sp) orbital, the number of electrons occupying the (5sp) orbital and c–f hybridization strength play an important role in the valence transition of $YbInCu_4$.

In summary, we have measured the He I high-resolution photoemission spectra of $YbXCu_4$ (X = In, Cd, Mg) in the wide binding energy region and near E_F from 10 to 300 K. The energy of the main peak due to the Cu 3d states is 3.1 eV for $YbInCu_4$ while 3.0 eV for $YbCdCu_4$ and $YbMgCu_4$. This slight difference is understood by taking into account the number of valence electrons of the In, Cd and Mg elements. The photoemission spectra of $YbInCu_4$ and $YbCdCu_4$ measured at 10 K exhibit the prominent peak due to the Yb^{2+} $4f_{7/2}$ states just below E_F. The Yb^{2+} $4f_{7/2}$ peak shows similar temperature dependence between $YbInCu_4$ and $YbCdCu_4$; with decreasing temperature from 300 to 50 K, the peak intensity increases and the peak energy shifts toward the E_F side. From 50 to 10 K, the temperature dependence of the Yb^{2+} $4f_{7/2}$ peak is different between the two compounds. The temperature dependence with respect to the enhancement of the peak intensity and the peak energy shift for $YbCdCu_4$ is monotonic down to 10 K, while in the case of $YbInCu_4$ the Yb^{2+} $4f_{7/2}$ peak is remarkably enhanced and the peak energy shifts slightly to the deeper-binding-energy side from 50 to 10 K. These remarkably different behaviours for $YbInCu_4$ would reflect the change of the valence-band electronic structure through the first-order valence transition at $T_v = 42$ K. On the other hand, the structure due to the Yb^{2+} $4f_{7/2}$ states of $YbMgCu_4$ is broad as a result of the strong hybridization between the Yb 4f and CB states, indicating that the electronic structure of $YbMgCu_4$ is extremely different from the other two compounds. However, the integrated Yb^{2+} $4f_{7/2}$ peak intensity increases with decreasing temperature, similar to the results of the two compounds. The Yb 4d photoemission spectra of $YbInCu_4$ and $YbCdCu_4$ indicate that the Yb^{2+} components increase gradually with decreasing temperature while the Yb^{3+} components decrease for both compounds. In particular, the Yb^{2+} component still exists at 300 K in $YbInCu_4$. The Yb atom in $YbMgCu_4$ is in the nearly divalent state. Although the Yb 4d spectrum of $YbMgCu_4$ is almost independent of temperature, the Yb^{3+}-derived structure is slightly observed at 300 K.

Acknowledgments

The authors are grateful to the Cryogenic Centre, Hiroshima University, for liquid helium. This work is partly supported by a Grant-in-Aid for Scientific Research from the Ministry of Education, Science and Culture, Japan.

References

[1] Sarrao J L *et al* 1999 *Phys. Rev.* B **59** 6855
[2] Sarrao J L 1999 *Physica* B **259–61** 128
[3] Felner I *et al* 1987 *Phys. Rev.* B **35** 6956
[4] Kojima K, Hayashi H, Minami A, Kasamatsu Y and Hihara T 1989 *J. Magn. Magn. Mater.* **81** 267
[5] Sarrao J L, Immer C D, Benton C L, Fisk Z, Lawrence J M, Mandrus D and Thompson J D 1996 *Phys. Rev.* B **54** 12 207
[6] Koskenmaki D C and Lawrence J M 1994 *Handbook on the Physics and Chemistry of Rare Earths* vol 19, ed K A Gschneidner, L Eyring, G H Lander and G R Choppin (Amsterdam: Elsevier) p 383
[7] Lawrence J M, Riseborough P S and Parks R D 1981 *Rep. Prog. Phys.* **44** 1
[8] Lawrence J M, Osborn R, Sarrao J L and Fisk Z 1999 *Phys. Rev.* B **59** 1134
[9] Very recently, a new theory for the valence transition of $YbIn_{1-x}Ag_xCu_4$ based on the lattice Anderson model has been proposed
Goltsev A V and Bruls G 2001 *Phys. Rev.* B **63** 155109
[10] Ogawa S, Suga S, Taniguchi M, Fujisawa M, Fujimori A, Shimizu T, Yasuoka H and Yoshioka K 1988 *Solid State Commun.* **67** 1093

[11] Okusawa M, Weschke E, Meier R, Kaindle G, Ishii T, Sato N and Komatsubara T 1996 *J. Electron. Spectrosc. Relat. Phenom.* **78** 139
[12] Reinert F, Claessen R, Nicolay G, Ehm D, Hüfner S, Ellis W P, Gweon G-H, Allen J W, Kindler B and Aßmus W 1998 *Phys. Rev.* B **58** 12 808
[13] Joyce J J, Arko A J, Sarrao J L, Graham K S, Fisk Z and Riseborough P S 1999 *Phil. Mag.* B **79** 1
[14] Moore D P, Joyce J J, Arko A J, Sarrao J L, Morales L, Höchst H and Chuang Y D 2000 *Phys. Rev.* B **62** 16 492
[15] Joyce J J, Arko A J, Morales L A, Sarrao J L and Höchst H 2001 *Phys. Rev.* B **63** 197101
[16] Reinert F, Claessen R, Nicolay G, Ehm D, Hüfner S, Ellis W P, Gweon G-H, Allen J W, Kindler B and Aßmus W 2001 *Phys. Rev.* B **63** 197102
[17] Kang J-S, Allen J W, Rossel C, Seaman C L and Maple M B 1990 *Phys. Rev.* B **41** 4078
[18] Weibel P, Grioni M, Malterre D, Dardel B, Bear Y and Besnus M J 1993 *Z. Phys.* B **91** 337
[19] Hiraoka K, Kojima K, Hihara T and Shinohara T 1995 *J. Magn. Magn. Mater.* **140–4** 1243
[20] Hiraoka K, Murakami K, Tomiyoshi S, Hihara T, Shinohara T and Kojima K 2000 *Physica* B **281/282** 173
[21] Takegahara K and Kasuya T 1990 *J. Phys. Soc. Japan* **59** 3299
[22] Tjeng L H *et al* 1993 *Phys. Rev. Lett.* **71** 1419
[23] Doniach S and Sunjic M 1970 *J. Phys. C: Solid State Phys.* **3** 285
[24] Joyce J J, Andrews A B, Arko A J, Bartlett R J, Blyth R I R, Olson C G, Benning P J, Canfield P C and Poirier D M 1996 *Phys. Rev.* B **54** 17 515
[25] Shirley D A 1972 *Phys. Rev.* B **5** 4709
[26] Blyth R I R *et al* 1993 *Phys. Rev.* B **48** 9497
[27] Yeh J J and Lindau I 1985 *At. Data Nucl. Data Tables* **32** 1
[28] Sato H *et al*, in preparation
[29] Chung J-S, Cho E-J and Oh S-J 1990 *Phys. Rev.* B **41** 5524